



LIBRARY

THE METEOROLOGICAL MAGAZINE

HER MAJESTY'S
STATIONERY
OFFICE

December 1981

Met.O. 942 No. 1313 Vol. 110

THE METEOROLOGICAL MAGAZINE

No. 1313, December 1981, Vol. 110

551.511.2:551.511.3:523.45

High-vorticity regions in rotating thermally driven flows*

By R. Hide, F.R.S.

(Meteorological Office, Bracknell)

Summary

The regular and irregular non-axisymmetric flow regimes of thermal convection in a rotating fluid annulus subject to differential heating in the horizontal are characterized by the presence of upper-level jet streams, where intense concentrations of vorticity and high concomitant horizontal temperature gradients are found. The main features of the upper-level flow pattern can be interpreted by straightforward arguments based on general thermodynamic considerations and the requirement that the flow should be quasi-geostrophic nearly everywhere. Thus, when the distribution of applied heating and cooling is such that the corresponding gradient of the impressed radial temperature field has the same sign at all radii, the most conspicuous feature of the upper-level flow pattern in the regular non-axisymmetric regime is a single jet stream meandering in a wavy pattern between the bounding cylinders. When, however, the impressed radial temperature gradient changes sign near mid-radius (as in the case when heat is introduced throughout the body of the fluid and withdrawn at both side-walls), the corresponding upper-level flow consists of several closed eddies, each circulating 'anticyclonically' with the horizontal flow largely confined to a narrow jet stream at the periphery of each eddy. In some respects these stable closed eddies are dynamically similar to long-lived anticyclonic eddies (including the Great Red Spot) seen in Jupiter's atmosphere in the southern hemisphere. Previous work on stable baroclinic eddies is now being extended in various directions and supporting numerical work is also being carried out.

1. Introduction

The motion of a fluid that departs but little from solid body rotation with angular velocity Ω is usually geostrophic nearly everywhere, with the relative Eulerian velocity \mathbf{u} (as measured in a frame of reference that rotates with angular velocity Ω relative to an inertial frame) satisfying

$$2\rho\Omega \times \mathbf{u} = -\nabla p + \rho\nabla V. \quad \dots \dots \dots (1)$$

* Invited paper presented at the joint International Union for Theoretical and Applied Mechanics/International Union for Geodesy and Geophysics symposium on *Intense Atmospheric Vortices*, 14–17 July 1981, European Centre for Medium-range Weather Forecasts, Shinfield Park, near Reading, England.

Here ρ denotes density, p denotes pressure and ∇V is the acceleration due to gravity and centripetal effects. Equation (1) is the leading approximation to the full equation of motion,

$$\rho \left(\frac{D\mathbf{u}}{Dt} + 2\boldsymbol{\Omega} \times \mathbf{u} - \mathbf{r} \times \frac{d\boldsymbol{\Omega}}{dt} \right) = -\nabla p + \rho \nabla V - \nabla \times (\nu \rho \nabla \times \mathbf{u}). \dots \dots (2)$$

It is valid in regions where the Coriolis term $2\rho\boldsymbol{\Omega} \times \mathbf{u}$ greatly exceeds the relative acceleration term $\rho D\mathbf{u}/Dt \equiv \rho(\partial\mathbf{u}/\partial t + \mathbf{u} \cdot \nabla \mathbf{u})$ (where t denotes time), the precessional term $\rho \mathbf{r} \times d\boldsymbol{\Omega}/dt$, the viscous term $\nabla \times (\nu \rho \nabla \times \mathbf{u})$ (where ν denotes kinematic viscosity) and any other term that must be added to equation (2) when further effects (e.g. magnetohydrodynamic forces) have to be taken into account.

Now equation (1) is lower in order than equation (2), so it cannot be solved under the complete set of boundary conditions. For this to be possible it is necessary to include every term in equation (2) in the analysis. It follows that the flow cannot be geostrophic everywhere; the system must exhibit boundary layers and detached shear layers where $\rho D\mathbf{u}/Dt + \nabla \times (\nu \rho \nabla \times \mathbf{u})$ is comparable in magnitude with $2\rho\boldsymbol{\Omega} \times \mathbf{u}$. Within these highly ageostrophic regions the magnitude of the relative vorticity $\nabla \times \mathbf{u}$ can be comparable with or even exceed $2\boldsymbol{\Omega}$. Many examples of such vorticity concentrations are found in laboratory systems and in nature. They are often associated with steep gradients of temperature (thermal fronts), as in the case of jet streams and western boundary currents found in atmospheres and oceans.

Jet streams are a pronounced feature of the non-axisymmetric flow regimes of thermal convection in a rotating fluid annulus, laboratory and theoretical studies of which have elucidated many aspects of the general circulation of the atmospheres of the Earth and other planets. This paper outlines the findings of work on annulus convection produced by internal heating and mentions one particularly interesting possible application (Hide 1980) to the interpretation of long-lived anticyclonic eddies (including the Great Red Spot) seen in Jupiter's atmosphere.

2. Sloping convection in the laboratory

Laboratory experiments in thermal convection in a rotating fluid annulus which rotates about a vertical axis and is subject to axisymmetric applied differential heating were initiated by the writer over 30 years ago (for references see Hide and Mason 1975, Pfeffer, Buzyna and Kung 1980, and Tritton and Davies 1981). They show that when the rotation rate $\boldsymbol{\Omega}$ exceeds a certain critical value $\boldsymbol{\Omega}_R$ (which depends on the acceleration due to gravity, the shape and dimensions of the apparatus, the coefficients of thermal expansion, thermal conductivity and viscosity of the fluid and its mean density, and the distribution and intensity of the applied differential heating, see section 4 below) Coriolis forces inhibit overturning motions in meridian planes and promote a completely different kind of motion, which has been termed 'sloping convection'. The motion is then non-axisymmetric and largely confined to jet streams, with typical trajectories of individual fluid elements inclined at only very small but essentially non-zero angles to the horizontal. The kinetic energy of the non-axisymmetric flow derives from the interaction of slight upward and downward motions in these sloping trajectories with the potential energy field produced by the action of gravity on the density variations maintained by the applied differential heating. The kinetic energy of the motion is dissipated by friction arising in boundary layers on the walls of the container and in the main body of the fluid.

Provided that $\boldsymbol{\Omega}$, though greater than $\boldsymbol{\Omega}_R$, does not exceed a second critical value $\boldsymbol{\Omega}_1$ (see section 4 below), the main features of the non-axisymmetric motion are characterized by great regularity. This regular flow is either steady (apart from a steady drift of the horizontal flow pattern relative to the walls of the apparatus) or it exhibits periodic 'vacillation' in the amplitude, shape and other characteristics. The number of 'waves' m around the annulus is not uniquely determined by the impressed conditions;

the flow is found to be 'intransitive' owing to the occurrence of what have come to be called 'multiple equilibrium states'. But a quantity m , defined as the most likely value of m at a point in the region of parameter space occupied by the regular flow regime (where $\Omega_R < \Omega < \Omega_I$, see Fig. 1), tends to increase with increasing Ω , until at $\Omega = \Omega_I$ the quantity m has that value for which the azimuthal scale of the horizontal flow pattern (namely the mean circumference of the annulus divided by m) is about 1.5 times the radial scale. Then the motion undergoes a transition to the so-called regime of irregular flow, where $\Omega > \Omega_I$ in parameter space, which is an example of thermally driven 'geostrophic turbulence'.

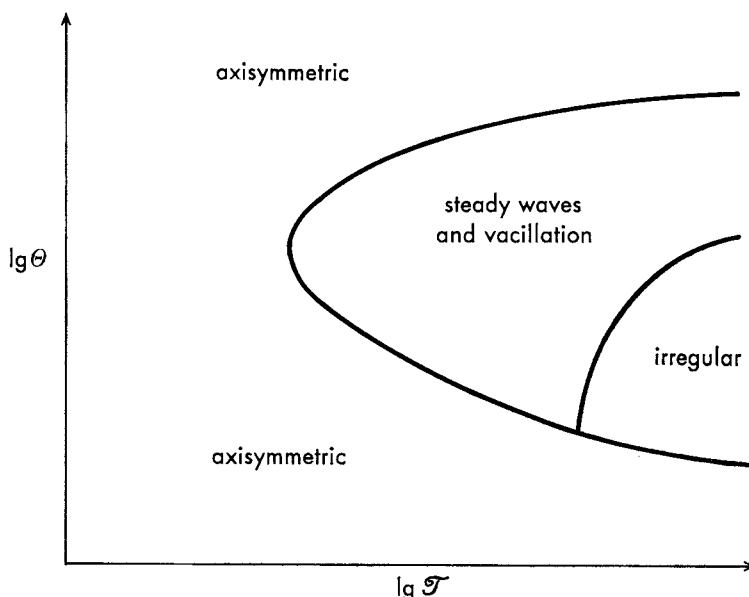


Figure 1. Schematic diagram illustrating the dependence of the mode of free thermal convection in a rotating fluid annulus under axisymmetric boundary conditions on the two dimensionless parameters found to specify the system, Θ and \mathcal{F} (see equations (12) and (13)).

Many laboratory studies of various aspects of sloping convection have now been carried out. These include measurements of heat transfer, flow structure and regime transitions over a wide range of mechanical and thermal boundary conditions. Numerical studies are playing an increasingly important role in this work, and significant if more limited analytical studies have been made based on the essentially non-linear governing mathematical equations.

These equations are the equations of motion (2), together with the equations of continuity and state for a liquid, respectively

$$\nabla \cdot \mathbf{u} = 0 \quad \dots \quad (3)$$

and

$$\rho = \rho_0 \{1 - \alpha(T - T_0)\} \quad \dots \quad (4)$$

where T denotes temperature, α denotes thermal coefficient of cubical expansion and ρ_0 is the density at the reference temperature T_0 , and the equation of heat transfer,

$$\frac{\partial T}{\partial t} + (\mathbf{u} \cdot \nabla) T = \kappa \nabla^2 T + q \quad \dots \quad (5)$$

where κ is the thermal diffusivity (equal to the thermal conductivity divided by the product of ρ and the specific heat capacity c) and $q\rho c$ is the rate of diabatic heating per unit volume. Across any cylindrical vertical surface $r = \text{a constant}$, where (r, ϕ, z) are cylindrical polar coordinates of a general point, $r = 0$ being the rotation axis (see Fig. 2), and the rate of heat transfer is given by

$$H(r, t) = \int_0^d \int_0^{2\pi} \rho c \left(\kappa \frac{\partial T}{\partial r} + u_r T \right) r \, d\phi \, dz \quad \dots \quad (6)$$

where the fluid extends in the axial direction from $z = 0$ to $z = d$. It is important to notice that the geostrophic contribution to the advective heat flow term on the right-hand side of equation (6) would vanish if the flow were axisymmetric, since by equation (1) u_r , the r component of $\mathbf{u} = (u_r, u_\phi, u_z)$, satisfies $u_r \doteq (2\rho\Omega r)^{-1} \partial p / \partial \phi$. This result points to the *raison d'être* of the non-axisymmetric regime of flow found when $\Omega > \Omega_R$; geostrophic flow cannot convey heat perpendicularly to the axis of rotation unless it is non-axisymmetric!

The boundary conditions on \mathbf{u} under which equations (2), (3), (4) and (5) must be satisfied are that $\mathbf{u} = 0$ at a rigid bounding surface and that the stress should vanish at a free surface. The thermal boundary conditions require continuity of heat flow which, at a bounding surface, is purely conductive and proportional to $\kappa \nabla T$. When the boundary conditions on the side-walls at $r = r^*$, where $r^* = a$ or b (say, with $b > a$, see section 4 below), are combined with the geostrophic relationship given by equation

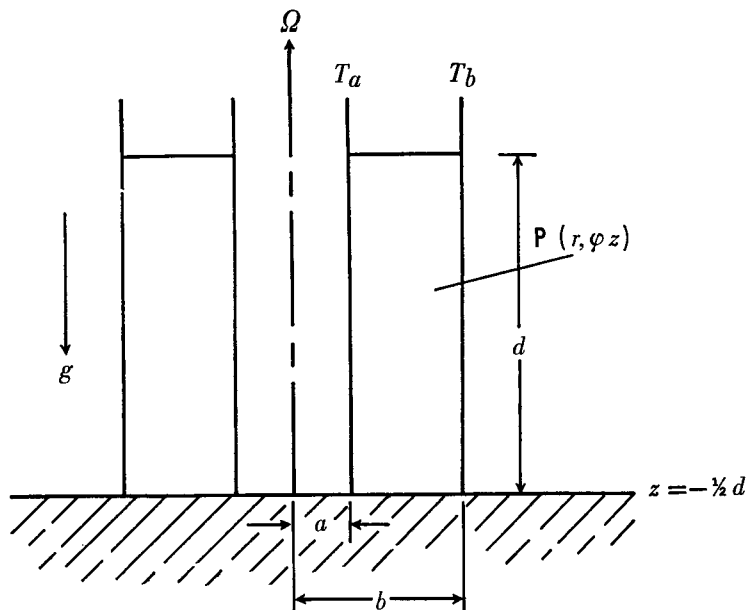


Figure 2. Schematic diagram of a rotating fluid annulus subject to a horizontal temperature gradient. (See Hide 1958 or Hide and Mason 1975 for further details.)

(1) and used in conjunction with the standard relationship for the radial flow in the Ekman boundary layers on $z = 0$ and $z = d$ to evaluate the radial heat flow at $r = r^*$ (see equation (6)), it is found (see Hide and Mason 1970) that:

$$H(r^*, t) \doteq - \left(\frac{\nu}{\Omega} \right)^{\frac{1}{2}} \left\{ \hat{T}(r^*, d, t) - \hat{T}(r^*, 0, t) \right\} \left\{ \Gamma(r^*, d, t) - \Gamma(r^*, 0, t) \right\}. \quad \dots \quad (7)$$

Here

$$\hat{T}(r^*, z, t) \equiv \frac{1}{2\pi} \int_0^{2\pi} T(r^*, \phi, z, t) d\phi \quad \dots \quad (8)$$

and

$$\Gamma(r^*, z, t) \equiv \int_0^{2\pi} U_\phi(r^*, \phi, z, t) r d\phi, \quad \dots \quad (9)$$

where $U_\phi(r^*, \phi, z, t)$ is the value of u_ϕ evaluated just outside the viscous boundary layer on $r = a$ or $r = b$, as the case may be. Now it may be shown that $\hat{T}(r^*, d, t) > \hat{T}(r^*, 0, t)$ (when $\alpha > 0$, see equation (4)) and that either $\Gamma(r^*, 0, t) = -\Gamma(r^*, d, t)$ or $|\Gamma(r^*, 0, t)| \ll |\Gamma(r^*, d, t)|$, according as the upper surface is in contact with a rigid lid or is free. Hence,

$$H(r^*, t) = (\text{negative definite quantity}) \times \Gamma(r^*, d, t). \quad \dots \quad (10)$$

This relationship between the heat flow at a side-wall and the line integral of the tangential velocity near the side-wall embodies the arguments used by Hide (1958) to provide a general interpretation of the upper-level flow pattern in the case when $q = 0$ everywhere (see equation (5)), heat being introduced into the system via one of the side-walls and removed via the other side-wall. The corresponding impressed radial temperature gradient has the same sign at all values of r and the upper-level pattern of motion in the regular flow regime consists of a single jet stream meandering in a wavy pattern between the bounding cylinders, with a positive (i.e. 'westerly') azimuthal component when heat enters via the outer side-wall and leaves via the inner side-wall (so that the impressed radial temperature gradient is positive) and a negative ('easterly') component when the radial heat transfer is in the opposite direction, from the inner to the outer cylinder (see Figs 3(a) and 3(b)).

As a further test of equation (10) Hide and Mason (1970) carried out experiments using internal heating, so that the term q in equation (5) is not equal to zero. This was done by passing an alternating electric current through the fluid. Heat could be removed via the inner side-wall, the outer side-wall or both side-walls. The observed upper-surface flow patterns (see Fig. 4) were found to be in good agreement with predictions for these three cases made on the basis of equation (10) (see Figs 3(c), (d) and (e)). In the cases where heat is removed via one side-wall only, $H(r^*, t)$ vanishes at the other side-wall and, by equation (10), the quantity $\Gamma(r^*, d, t)$ must also vanish. For this to happen, $U_\phi(r^*, \phi, d, t)$ will be positive at some values of ϕ and negative at others (or zero at all values of ϕ , as in the axisymmetric regime that occurs when $\Omega < \Omega_R$). Figs 3(c) and (d) show how this requirement can be satisfied by adding closed eddies to the wavy pattern found in the cases when $q = 0$ (cf. Figs 3(a) and (b)).

The most striking case of all studied in the experiments is the one illustrated by Fig. 3(e). Then, heat is removed via both side-walls, implying that the impressed radial temperature gradient changes sign near mid-radius. The corresponding upper-level flow consists of several separate closed eddies each circulating anticyclonically, in accordance with equation (10), with the horizontal flow confined to a narrow jet stream at the periphery of each eddy (see Fig. 4(c)).

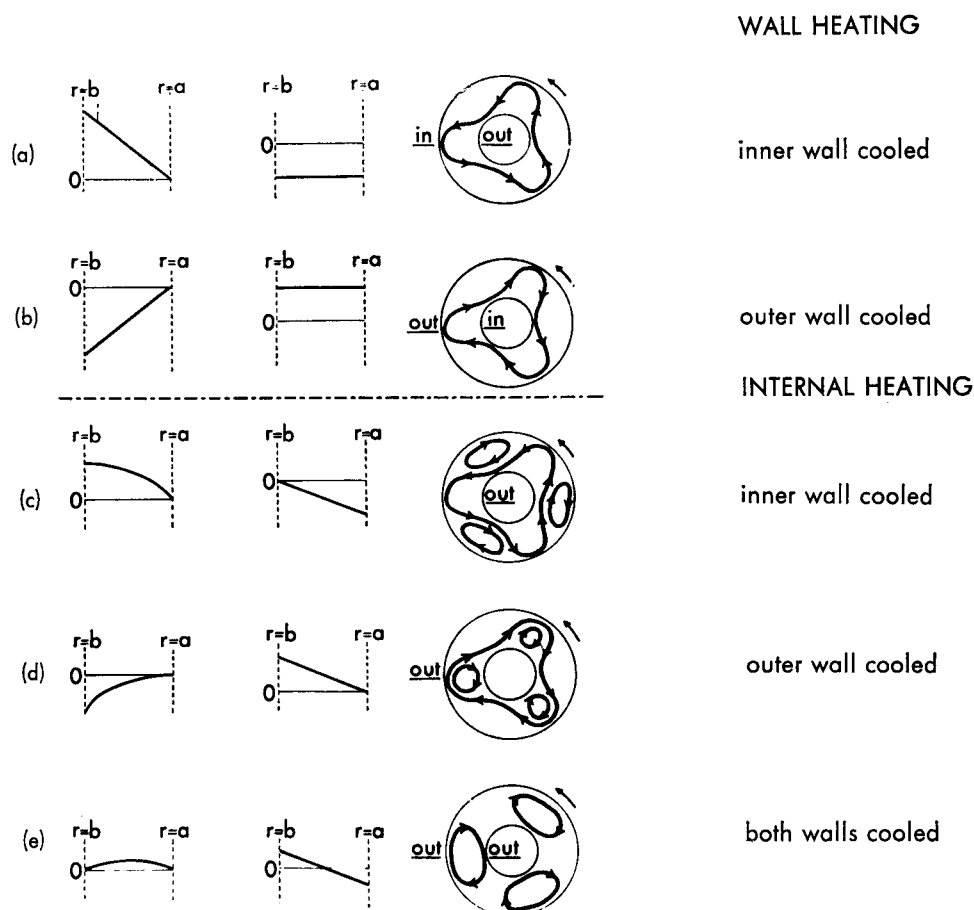


Figure 3. Schematic illustrations of the radial variation of the impressed temperature (left column), of the radial variation of the impressed radial temperature gradient (middle column), and of the corresponding upper-surface relative flow pattern in the regular regime of thermal convection in a rotating fluid annulus (right column), as predicted on the basis of equation (10). (See Hide and Mason 1970 for further details.)

3. Atmospheric flows

The meandering jet streams within which the upper-level tropospheric air flow is mainly concentrated in the Earth's atmosphere are manifestations of sloping convection produced by differential solar heating, which maintains a systematic temperature contrast between tropical and polar regions in each hemisphere. These atmospheric motions are much less regular than those depicted in Figs 3(a), 3(c) and 4(a) (cf. Fig. 5), presumably because the Earth's angular speed of rotation exceeds the critical value Ω_c , although horizontal variations of surface conditions introduce complications which are not yet fully understood.

The atmosphere of the planet Jupiter is heated from below at about the same rate as its upper reaches are heated by solar radiation. Unlike the terrestrial case (where non-solar atmospheric heating is utterly negligible), north-south temperature gradients in Jupiter's atmosphere change sign several times between equator and pole and there is no evidence of any significant systematic temperature contrast

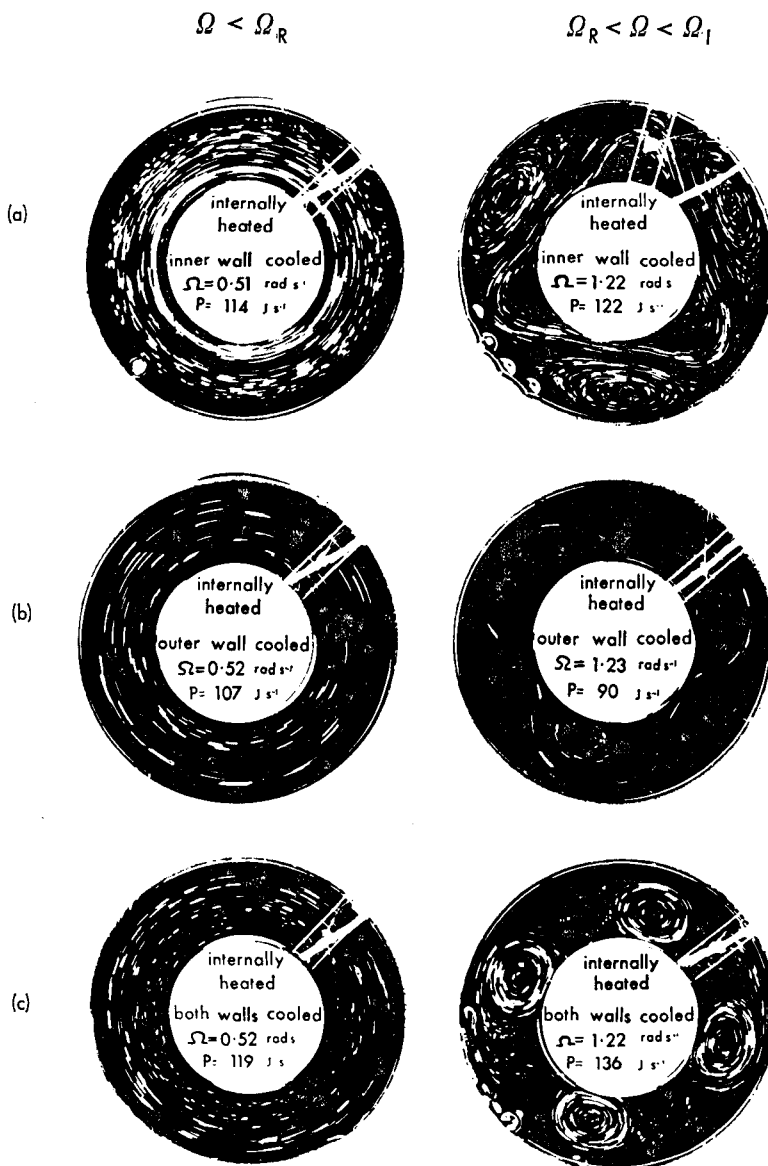


Figure 4. Streak photographs illustrating top-surface flow patterns of thermal convection in a rotating fluid annulus subject to internal heating in the axisymmetric regime (when $\Omega < \Omega_R$, see left column) and regular non-axisymmetric regime (when $\Omega_R < \Omega < \Omega_I$, see right column). They show the dependence of the general characteristics of the flow pattern on the way heat is removed from the system and confirm predictions based on equation (10). The cases (a), (b) and (c) correspond to cases (c), (d) and (e) respectively in Fig. 3. In the most striking case of all (see Figs 3(e) and 4(c)) sloping convection takes the form of closed anticyclonic eddies with the main motion concentrated in a jet stream at the periphery of each eddy. (See Hide and Mason 1970 for further details.)

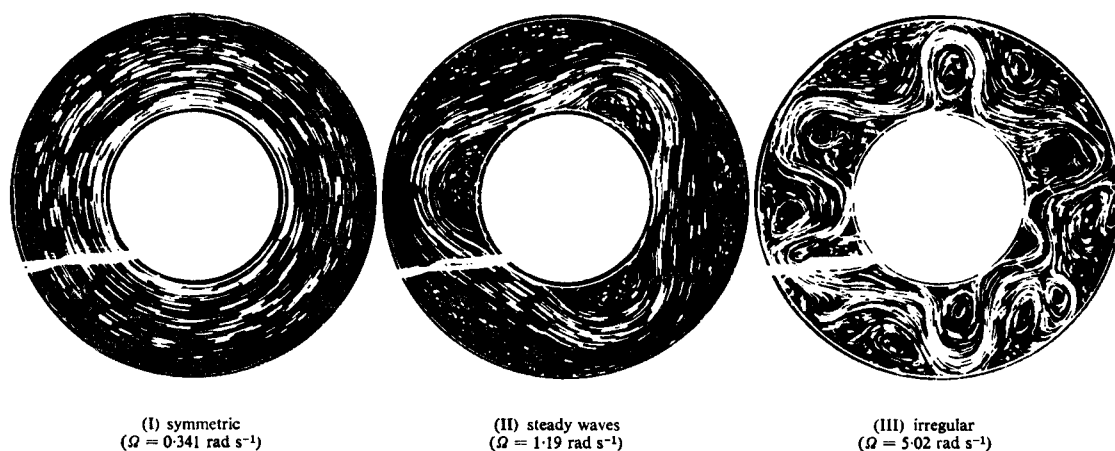


Figure 5. Streak photographs giving one example of each of the main modes of thermal convection in a rotating fluid annulus subject to a radial temperature field of the form given by equation (11), namely (I) axisymmetric flow, (II) regular (steady) non-axisymmetric flow, and (III) irregular non-axisymmetric flow.

between equatorial and polar regions (for references see Ingersoll, Dobrovolskis and Jakosky 1979). There are abundant observations of Jovian atmospheric motions at the upper-cloud level, some of which go back many decades and even longer, and the Pioneer and Voyager space probes have added further details (see Peek 1958, Smith and Hunt 1976, NASA 1979 and Mitchell *et al.* 1981). Our knowledge of what goes on below the cloud level is meagre and this produces difficulties with the interpretation of observations of upper-level atmospheric motions. Indeed, it has been argued elsewhere that the main task of the 'Jovian meteorologist' should perhaps be to use these observations to improve our knowledge of the vertical structure of the planet (see e.g. Hide 1981).

But here is not the place to discuss these observations and review the many interesting though largely controversial issues being debated by those of us who take an interest in the interpretation of the observations in terms of basic dynamical processes. There is, however, one striking phenomenon upon which laboratory experiments on sloping convection in a fluid annulus subject to internal heating might have some bearing. The highly stable closed anticyclonic eddies with the main motion concentrated in a jet stream at the periphery of each eddy that are depicted in Figs 3(e) and 4(c) are remarkably similar dynamically to the long-lived eddies to be seen in Jupiter's atmosphere in the southern hemisphere. The largest, oldest and most conspicuous of these is the Great Red Spot in the South Tropical Zone which may be at least 300 years old. Next in size and age are the three White Ovals that formed in 1939 at the boundary between the South Temperate Belt and the South Temperate Zone, apparently as the residue of the highly irregular South Tropical Disturbance that was first seen in 1901. The smallest of the long-lived eddies are clearly seen in the magnificent Voyager pictures (NASA 1979) as about a dozen oval markings somewhat closer to the pole. The motion in each of these Jovian eddies is anticyclonic and largely confined to a narrow region at the edge of the eddy. It is tempting therefore to suppose (Hide 1980) that the eddies are manifestations of sloping convection in Jupiter's atmosphere, implying that they derive their kinetic energy directly from the potential energy due to the action of gravity on density variations produced by internal and solar heating and that they transport heat from the interior to the edges of the latitudinal bands in which they arise. (See Plate I.)

Preliminary calculations indicate that there is nothing unreasonable about this hypothesis so far as its implications for the vertical structure and other properties of Jupiter's atmosphere are concerned, but a

detailed examination of these implications and a critical comparison of the hypothesis with other proposals as to the nature of the long-lived anticyclonic eddies will have to be considered elsewhere. The hypothesis raises a number of fluid-dynamical questions to be resolved by further laboratory and numerical work and some of this is now in hand. Amongst these questions is that of the instability of the strongly sheared flow in the jet stream itself. Experiments with a wall-heated annulus (Hide 1958) provide some evidence that when viscous effects are sufficiently small the jet stream develops local instabilities on one side but not on the other. Pictures of Jupiter show highly irregular flow on a comparatively small scale just outside the Great Red Spot (and the other long-lived eddies), but not on the inside. It will be important to establish by experiment and theory (cf. Narasimha 1980) whether this highly irregular flow arises as a result of a 'one-sided' instability of the jet stream at the edge of the main eddy.

4. Appendix: Regimes of thermal convection in a rotating fluid annulus

The simplest system in which controlled and reproducible experiments on sloping convection have been carried out is the annular apparatus illustrated in Fig. 2 when there are no internal sources of heat (i.e. $q = 0$, see equation (5)) but the bounding cylindrical side-walls in $r = a$ and $r = b$ are maintained at different temperatures T_a and T_b respectively, so that the impressed temperature field satisfies

$$T_i = \{T_b \ln(r/a) - T_a \ln(r/b)\} / \ln(b/a), \quad \dots \dots \dots (11)$$

which simplifies to $T_i = \frac{1}{2}(T_b + T_a) + (T_b - T_a) \{r - \frac{1}{2}(a + b)\} / (b - a)$ when $(b - a) \ll \frac{1}{2}(b + a)$. Accurate determinations of the principal spatial and temporal characteristics of the fields of temperature and flow velocity over a wide range of precisely specified and carefully controlled experimental conditions led to the discovery of several fundamentally different free types of flow, only one of which is symmetrical about the axis of rotation (see Figs 5 and 6). The general character of the flow evidently depends largely on the values of certain external dimensionless parameters,

$$\Theta \equiv g d \Delta \rho / \bar{\rho} \Omega^2 (b - a)^2 \quad \dots \dots \dots (12)$$

and

$$\mathcal{F} \equiv 4 \Omega^2 L^4 / \nu^2 \dots \dots \dots (13)$$

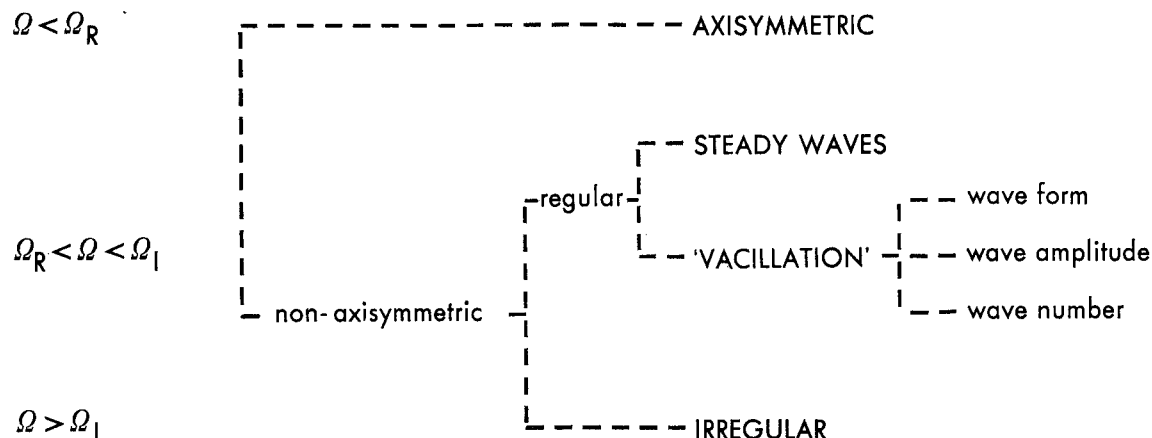


Figure 6. Broad classification of modes of free thermal convection in a rotating fluid annulus under axisymmetric boundary conditions. (See Hide 1958 or Hide and Mason 1975 for further details.)

Here g denotes the acceleration due to gravity (which is typically very much greater than $\Omega^2 b$), d is the depth of the liquid in the annular container, $\Delta\rho$ is the density contrast associated with the impressed temperature difference, i.e. $|\rho(T_a) - \rho(T_b)|$, $\bar{\rho}$ is the mean density, Ω is the angular speed of rotation of the apparatus about a vertical axis, ν is the kinematic viscosity and L , which has the dimensions of a length, is equal to $(b - a)^{5/4}/d^{1/4}$ over a wide range of conditions.

When \mathcal{T} is less than a certain critical value of about 2×10^5 (see Fig. 1), viscosity ensures that the motion is essentially symmetrical about the axis of rotation for all values of Θ . However, when \mathcal{T} exceeds this critical value there exists a range of Θ within which highly non-axisymmetric sloping convection occurs. These non-axisymmetric motions are either regular or irregular (see Fig. 5) depending on the values of Θ and \mathcal{T} . The regular flows often exhibit periodic 'vacillation' in amplitude, shape or wavenumber, but under certain conditions these periodic variations are so slight that, apart from a steady drift of the wavy pattern relative to the apparatus, the flow is virtually steady. In sharp contrast to this behaviour, the irregular flows exhibit complicated aperiodic fluctuations in both space and time.

Consider an experiment in which all the impressed conditions are kept fixed except Ω , which is increased in steps from low values to high values. This can be represented by a series of points on a straight line inclined at 45° to the \mathcal{T} and Θ axes in the regime diagram of Fig. 1, moving from the upper left part of the diagram to the lower right. The critical value Ω_R of Ω corresponds to the point where the transition from axisymmetric to regular non-axisymmetric flow occurs and the critical value Ω_I to the point where the transition from regular to irregular non-axisymmetric flow occurs.

References

- | | | |
|--|------|--|
| Hide, R. | 1958 | An experimental study of thermal convection in a rotating liquid. <i>Philos Trans R Soc, London, A</i> , 250 , 441–478. (For further details see Hide, R., Ph.D. dissertation, Cambridge University, 1953.) |
| | 1980 | Jupiter and Saturn: giant magnetic rotating fluid planets. <i>Observatory</i> , 100 , 182–193. |
| | 1981 | On the rotation of Jupiter. <i>Geophys J R Astron Soc</i> , 64 , 283–289. |
| Hide, R. and Mason, P. J. | 1970 | Baroclinic waves in a rotating fluid subject to internal heating. <i>Philos Trans R Soc, London, A</i> , 268 , 201–232. |
| | 1975 | Sloping convection in a rotating fluid. <i>Adv Phys</i> , 24 , 47–100. |
| Ingersoll, A. P., Dobrovolskis, A. R. and Jakosky, B. M. | 1979 | Planetary atmospheres. <i>Rev Geophys Space Phys</i> , 17 , 1722–1735. |
| Mitchell, J. L., Beebe, R. F., Ingersoll, A. P. and Garneau, G. W. | 1981 | Flow fields within Jupiter's Great Red Spot and White Oval BC. <i>J Geophys Res</i> (in press). |
| Narasimha, R. | 1980 | The possible influence of curvature and rotation on ocean currents. <i>Proc Indian Acad Sci (Earth Planet Sci)</i> , 89 , 267–275. |
| NASA | 1979 | Voyager encounters Jupiter. Washington, D.C., National Aeronautics and Space Administration. |
| Peek, B. M. | 1958 | The planet Jupiter. London, Faber. |
| Pfeffer, R. L., Buzyna, G. and Kung, R. | 1980 | Time-dependent modes of behaviour of thermally driven rotating fluids. <i>J Atmos Sci</i> , 37 , 2129–2149. |
| Smith, B. A. and Hunt, G. E. | 1976 | Motions and morphology of clouds in the atmosphere of Jupiter. In Gehrels, T. (ed.), <i>Jupiter: studies of the interior, atmosphere, magnetosphere and satellites</i> . Tucson, University of Arizona Press. |
| Tritton, D. J. and Davies, P. A. | 1981 | Instabilities in geophysical fluid dynamics. In Swinney, H. L. and Gollub, J. P. (eds), <i>Hydrodynamic instabilities and the transition to turbulence</i> . Berlin, Heidelberg, New York, Springer-Verlag. |

Meteosat water vapour imagery

By J. R. Eyre

(Meteorological Office, Bracknell)

Summary

The Meteosat radiometer includes a channel for measuring radiation emitted mainly by water vapour in the middle and upper troposphere. The interpretation of images produced by this instrument is discussed and applications, both quantitative and qualitative, for the data obtained from the water vapour channel are reviewed.

1. Introduction

Radiometers carried on meteorological satellites can be considered as divided into two types—imagers and sounders. Conventional imaging instruments operate at wavelengths for which the atmospheric absorption is low and provide ‘pictures’ of the underlying surfaces—land, sea or cloud top—with very little atmospheric attenuation. Examples of such instruments on recent satellites are the visible and infra-red channels of the Advanced Very High Resolution Radiometer (AVHRR) on the TIROS-N series (Schwalb 1978), which has a resolution of *c.* 1 km, and the visible (VIS) and 11 μm infra-red (IR) channels of Meteosat, which have respective resolutions of *c.* 2.5 km and *c.* 5 km at the sub-satellite point (European Space Agency 1978). On the other hand, the wavelengths used by sounding instruments are such that most of the radiation measured has been emitted by the atmosphere itself. Emission from gases of known concentration, such as carbon dioxide and oxygen, can be used to estimate atmospheric temperature, while information on the variable concentration profiles of constituents such as water vapour can be deduced from measurements at the wavelengths of their absorption bands. The High-resolution Infra-Red Sounder (HIRS) on the TIROS-N series is an example of this type of instrument (Schwalb 1978, Smith *et al.* 1979). It has three channels principally for sounding tropospheric water vapour with a horizontal resolution of about 30 km.

However, the distinction between imagers and sounders cannot be carried too far, since the data from sounding instruments can often be built up into images (though usually with a resolution inferior to that of conventional imagers). In this way water vapour sounding channels can produce ‘water vapour images’, which provide opportunities for studies of atmospheric motions not previously available. Sounding instruments on several satellites have yielded water vapour images in the 6.3 μm water vapour band. (See, for example, Martin and Salomonson 1970, Steranka *et al.* 1973 and Kästner *et al.* 1980.) The Meteosat 6.3 μm water vapour (WV) channel possesses sounding characteristics similar to those of 6.3 μm channels on earlier satellites, sensing radiation emitted mainly by water vapour in the middle and upper troposphere. In addition it provides images of high horizontal resolution equal to that of the IR channel and was the first such channel to be used on a geostationary satellite (Morel *et al.* 1978). An example of a Meteosat WV image is given in Plate II.

2. Radiative transfer theory for the Meteosat WV channel

The radiance emitted at the top of a non-scattering atmosphere at zenith angle θ and wave number ν is given by the radiative transfer equation:

$$R_\nu = (I_0)_\nu \tau(\nu, \theta, z_s) + \int_{z_s}^{\infty} B\{\nu, T(z)\} \frac{d\tau(\nu, \theta, z)}{dz} dz \quad \dots \quad (2.1)$$

$$= (I_0)_\nu \tau(\nu, \theta, z_s) + \int_{z_s}^{\infty} B\{\nu, T(z)\} K(\nu, \theta, z) dz \quad \dots \quad (2.2)$$

$$= (I_0)_\nu \tau(\nu, \theta, z_s) + \int_{z_s}^{\infty} C(\nu, \theta, z) dz \quad \dots \quad (2.3)$$

$B\{\nu, T(z)\}$ is the Planck function corresponding to the atmospheric temperature $T(z)$ at height z and is given by

$$B\{\nu, T(z)\} = \frac{c_1 \nu^3}{\exp\{c_2 \nu / T(z)\} - 1},$$

where c_1 and c_2 are constants. $\tau(\nu, \theta, z)$ is the transmittance of an atmospheric path at zenith angle θ from height z to space, $(I_0)_\nu$ is the radiance from the surface (land, sea or cloud top), and the integration is performed from the surface at height z_s to space.

In (2.2) we have defined a 'weighting function', $K = d\tau/dz$, and in (2.3) we have defined a 'contribution function', $C = BK$. It can be seen that the second term in these equations is a weighted integral of the Planck function profile and that the appropriate weighting is given by K , the derivative of the transmittance profile with respect to height.

$\tau(\nu, \theta, z)$ is related to the concentration of absorbing gas by the equation,

$$\tau(\nu, \theta, z) = \exp\left\{-\sec \theta \int_z^{\infty} k(\nu, z) c(z) \rho(z) dz\right\}, \quad \dots \quad (2.4)$$

where $k(\nu, z)$ is the absorption coefficient, $c(z)$ is the mass mixing ratio profile and $\rho(z)$ is the atmospheric density profile.

In spectral regions sensed by the Meteosat WV channel ($c. 1400-1750 \text{ cm}^{-1}$) the dominant absorbing gas is water vapour. Therefore the transmittance profile and hence the weighting and contribution functions depend on the vertical humidity profile through (2.4). This is illustrated in Fig. 1 for an atmosphere of standard temperature profile and three different values of tropospheric relative humidity. The curves shown represent values appropriately averaged over the WV channel spectral pass-band. It can be seen that for a given temperature profile an increase in humidity decreases the transmittance to space and so raises the height of the weighting function peak. In most cases the temperature profile decreases monotonically with height in the region of the weighting function and so the result of an increase in humidity is a decrease in the measured radiance, conventionally shown by a lighter shade of grey on the image. Therefore the WV channel radiance can be used to estimate the humidity of the middle and upper troposphere (if the temperature profile is known). The images can also be used qualitatively to identify areas of high and low relative humidity (light and dark shades of grey respectively).

If the underlying surface is below about 800 mb, then for the majority of atmospheric profiles the first term in (2.1) may be neglected. However, if there is cloud at levels around or above the peak of the cloud-free weighting functions, then the cloud top will make a significant contribution to the radiance. For this reason high clouds such as cirrus and cumulonimbus tops stand out on the WV image as they would on the IR image, but low-level clouds do not appear.

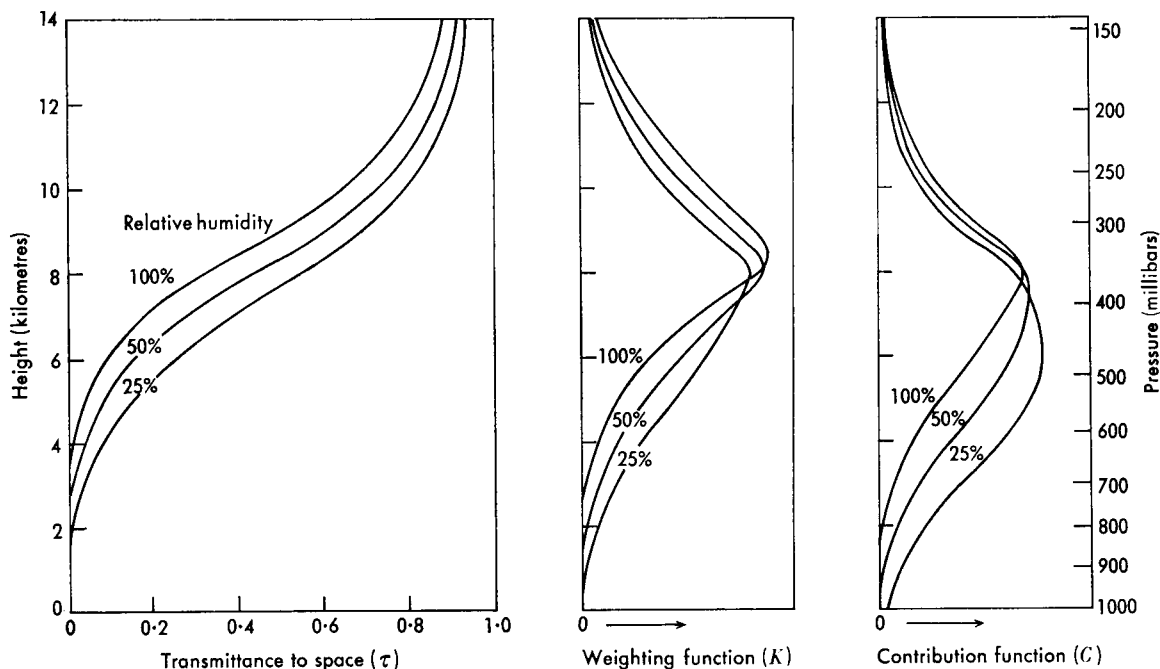


Figure 1. Meteosat water vapour channel transmittance, weighting function and contribution function for a range of relative humidities.

3. Quantitative uses of Meteosat WV channel data

(a) Humidity of the upper troposphere

The radiative transfer theory given above defines the relationship between radiance and humidity. From one radiance only it is not possible to retrieve a complete vertical humidity profile, but we can use it to estimate the mean relative humidity of the upper troposphere. This is the approach to be used by the European Space Operations Centre (ESOC) at Darmstadt to derive the Meteosat 'upper tropospheric humidity product' (European Space Agency 1980) and it has been used with $6.3 \mu\text{m}$ data from other satellites to estimate global water vapour budgets (e.g. Raschke and Bandeen 1967). An example of ESOC's product is shown in Fig. 2.

An alternative approach is to use a humidity profile forecast by a numerical model as a first guess and to adjust this profile until it gives agreement with the measured radiance. This method is being investigated at the Meteorological Office, using Meteosat WV channel data (Eyre 1981). Similar methods can be applied to other water vapour sounding channels such as those of HIRS.

the WV image (Kästner *et al.* 1980, Eigenwillig and Fischer 1980). In cloud-free regions such features represent horizontal gradients in the humidity field. By tracking them and assuming that they move with the wind speed, horizontal winds in the clear air can be estimated. Difficulties arise because the Meteosat WV image is noisier than the IR image and also because the clear-air water vapour structures tend to be less clearly defined—they do not have sharp edges in the WV image. These characteristics adversely affect the calculation of motion vectors by automatic pattern correlation techniques. Also, the motion vectors calculated correspond to the average winds of rather broad layers represented by the contribution functions.

The WV channel radiances have also been used operationally in the process of assigning heights to semi-transparent high cloud tracked using the IR image since, for reasons given above, the IR radiance alone does not lead to accurate height assignment in such cases.

(c) *Vertical motion*

If it is possible to track a clear-air feature from one image to another, then the small change in the mean radiance of the feature can be used to estimate the mean vertical motion (Rodgers *et al.* 1976, Eyre 1980). If we can assume that water vapour is a conservative tracer of the motion and neglect wind shear effects, then the change in the contribution to the radiance from each element of the atmosphere is caused mainly by the change in temperature associated with the adiabatic compression or expansion which it experiences during vertical motion. Retrieval of such information is limited to areas where clear-air horizontal motion vectors have been accurately calculated and difficulties arise because large-scale mean vertical velocities in the atmosphere are never greater than a few cm s^{-1} . (1 cm s^{-1} corresponds to a change in WV channel brightness temperature of about 0.4 K h^{-1} .)

4. Qualitative uses of Meteosat WV channel data

None of the quantitative products given above was produced operationally from Meteosat 1 WV channel data. However, the images have been used qualitatively in a number of ways. They add to the data from other channels and other satellites which are available to forecasters, and since they represent radiation originating in the middle layers of the atmosphere they provide useful information on the flow patterns at these altitudes and often reveal features not apparent in conventional imagery or other meteorological observations.

At present our understanding of the synoptic interpretation of features in the WV imagery is limited. Upper tropospheric vortices can be seen and readily interpreted (Houghton and Suomi 1978). Also the long waves in the flow are usually evident from the bands in the image—bands which are often continuous over thousands of kilometres and identifiable for many days. However, a more careful analysis is required here since these bands cannot be directly associated with streamlines. Since in the clear air the water vapour is a conservative tracer of the motion, a band usually contains air originating from the same air mass. The band has been created and distorted by the divergence of the trajectories and in this way shows the recent history of the flow. Thus sequences of images reveal trajectories but a single image does not necessarily show the instantaneous flow. In addition, parts of the band will change in brightness because of vertical motion, as explained above. This complicates the interpretation but also provides qualitative information on the vertical motion field.

Of particular interest in WV images are narrow, dark bands in high and mid-latitudes associated with jet streams (Martin and Salomonson 1970, Ramond and Tjasyono 1979). Their darkness indicates that we are 'seeing' comparatively deep into the troposphere and confirms the existence of very dry bands of

air, often of stratospheric origin, which have descended on the poleward side of a jet stream. Thus the images provide a new source of data for studying the development and dynamics of jet streams and can be used operationally for jet stream location.

An example of such a dark band is shown across England in the WV image of 1230 GMT on 15 August 1978 (Plate III). The jet core was around 250 mb, and the 1200 GMT 250 mb analysis is shown for comparison in Fig. 3. It can be seen that the conventional analysis is in good agreement, with respect to both the position and shape of the jet, with the assumption that the jet axis lies close to the southern edge of the dark band. In fact it may be possible in such cases to deduce the details of the jet more accurately from the WV image than from the limited number of wind observations available, even where the conventional observing network is good. In data-sparse areas the image is obviously of even greater value. For the case given here the corresponding VIS and IR images did not give a clear indication of the jet stream position.

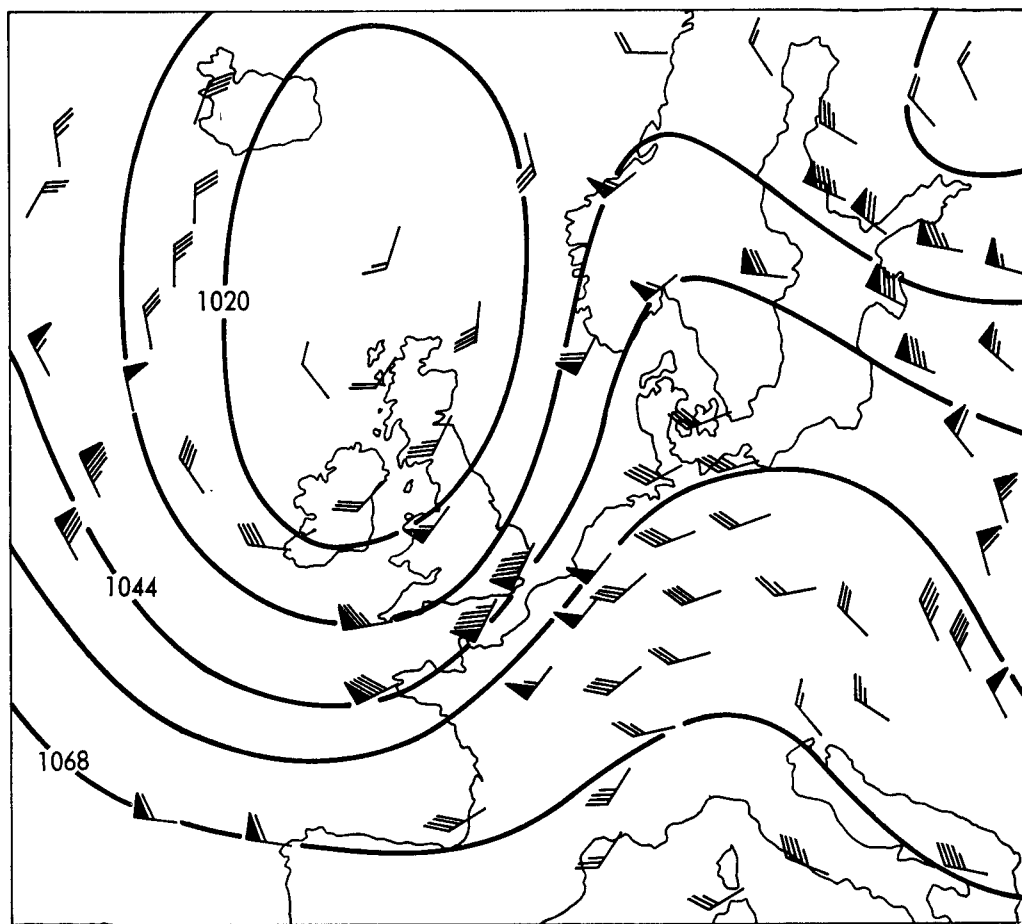


Figure 3. 250 mb analysis for 1200 GMT on 15 August 1978 (isopleths in decageopotential metres, wind speeds in knots).

5. Concluding remarks

The water vapour channel on Meteosat 1 was a considerable success, providing data of a new kind with applications in operational forecasting and research. The value of this channel on future satellites is likely to be greater still as our skill in interpreting the imagery improves and methods are developed for extracting useful products from the data.

References

- | | | |
|--|------|--|
| Cayla, F. R. and Tomassini, C. | 1978 | Détermination de la température des cirrus semi-transparents. <i>La Météorologie</i> , VIe Série, No. 15, 63–67. |
| Eigenwillig, N. and Fischer, H. | 1980 | Determination of wind vectors from Meteosat water vapour channel data. Second Meteosat Scientific User Meeting, London, 26–27 March 1980. |
| European Space Agency | 1978 | Introduction to the Meteosat system, issue 2. Darmstadt, ESA. |
| Eyre, J. R. | 1980 | Meteosat system guide. Darmstadt, ESA. |
| | 1980 | Calibration and some exploratory uses of Meteosat water vapour channel imagery. Second Meteosat Scientific User Meeting, London, 26–27 March 1980. |
| | 1981 | Improvement of humidity analyses by direct use of Meteosat water vapour channel radiances. Proceedings of IAMAP Symposium, Hamburg, 25–28 August 1981. |
| Houghton, D. D. and Suomi, V. E. | 1978 | Information content of satellite images. <i>Bull Am Meteorol Soc</i> , 59 , 1614–1617. |
| Kästner, M., Fischer, H. and Bolle, H.-J. | 1980 | Wind determination from Nimbus 5 measurements in the 6.3 μm water vapour band. <i>J Appl Meteorol</i> , 19 , 409–418. |
| Martin, F. L. and Salomonson, V. V. | 1970 | Statistical characteristics of subtropical jet-stream features in terms of MRIR observations from Nimbus II. <i>J Appl Meteorol</i> , 9 , 508–520. |
| Morel, P., Desbois, M. and Szejwach, G. | 1978 | A new insight into the troposphere with the water vapour channel of Meteosat. <i>Bull Am Meteorol Soc</i> , 59 , 711–714. |
| Ramond, D. and Tjasyono, B. | 1979 | Contribution à l'interprétation météorologique de l'imagerie fournie par le canal 6.3 μm de Meteosat aux moyennes latitudes. Institut et Observatoire de Physique du Globe du Puy-de-Dôme, <i>Note IOPG</i> 56. |
| Raschke, E. and Bandeen, W. R. | 1967 | A quasi-global analysis of tropospheric water vapour content from TIROS IV radiation data. <i>J Appl Meteorol</i> , 6 , 468–481. |
| Rodgers, E. B., Salomonson, V. V. and Kyle, H. L. | 1976 | Upper tropospheric dynamics as reflected in Nimbus 4 THIR 6.7 μm data. <i>J Geophys Res</i> , 81 , 5749–5758. |
| Schwalb, A. | 1978 | The TIROS-N/NOAA A-G satellite series. Washington, National Oceanic and Atmospheric Administration, National Environmental Satellite Service, <i>Tech Memo</i> , NESS 95. |
| Smith, W. L., Woolf, H. M., Hayden, C. M., Wark, D. Q. and McMillin, L. M. | 1979 | The TIROS-N operational vertical sounder. <i>Bull Am Meteorol Soc</i> , 60 , 1177–1187. |
| Steranka, J., Allison, L. J. and Salomonson, V. V. | 1973 | Applications of Nimbus 4 THIR 6.7 μm observations to regional and global moisture and wind field analyses. <i>J Appl Meteorol</i> , 12 , 386–395. |

551.5(09): 551.507.321.2

One hundred years ago: a ballooning tragedy

By R. P. W. Lewis

(Meteorological Office, Bracknell)

On 13 December 1881 Robert H. Scott, Secretary to the Meteorological Council, wrote to the War Office as follows:

I REGRET to have to inform you that on Saturday last the balloon "Saladin" was caught by a gust of wind on the coast at Bridport, broke away, and was carried out to sea.*

I enclose a copy of a report of the occurrence by Captain Templer, from which you will see that the balloon when it escaped carried with it Mr. W. Powell, M.P., who had been assisting Captain Templer in making the observations.

Up to the present time no tidings have been obtained of the balloon or its occupant.

The second half of the nineteenth century was the heroic age of exploration of the upper air when scientists ascended in manned balloons in conditions that were usually unpredictable and often dangerous. Glaisher and Coxwell, in their ascent made in 1862 for the British Association, were lucky to escape with their lives when their balloon ascended to over 30 000 feet and the cord controlling the release valve became tangled. In 1879 Captain James Templer, then of the Royal Middlesex Rifles, who was an experienced balloonist and was engaged in making experimental ascents both privately and on behalf of the War Office, expressed to the Meteorological Council his wish to make these ascents useful to meteorological science in any way he could. The Council accepted his offer, negotiated with the War Office for the loan of a suitable balloon, and sent Captain Templer a memorandum stating exactly what observations and measurements he ought to make. In the summer of 1881 the balloon 'Saladin' was available, and arrangements were made for Captain Templer to undertake several ascents, his expenses being paid by the Council.

In a full and detailed account of the ascent that ended in disaster, addressed to the Council, Captain Templer wrote:

On Friday, the 9th instant, London being enveloped in a very peculiar fog, I was anxious to ascertain the atmospheric conditions which might have produced it. On that day I was unfortunately detained in the train by the fog, but I determined to make the ascent on the following day, Saturday, December 10th. The balloon "Saladin" was at Bath, so I wrote to you that I would ascend from that place. I took Mr. Walter Powell as my assistant, for the management of the balloon.

Captain Templer had previously written to Dr R. H. Scott as follows:

SIR,

I REGRET to report that on Saturday, the 10th of December, I ascended at Bath, accompanied by Mr. Walter Powell and Mr. Agg Gardner, at 1h. 55m., for the purpose of taking the temperature of the air, and the amount of snow in the air, for the Meteorological Office. I cleared the snow clouds at 4,000 feet altitude; the temperature of these clouds was 28°, and the wet-bulb thermometer read 26°. At 4,200 feet we passed over Wells, the time being 2h. 50m. At this height I worked over Glastonbury; the temperature now rose to 41°, and the sky was perfectly clear. I passed then between Somerton and Landport, and I here found that I was in a N. $\frac{1}{2}$ W. current. I asked Mr. Powell to send the balloon up to 6,000 feet, to ascertain the temperature of a small bank of cirrus. I found this temperature to be 31°, and then I asked

* The *Daily Weather Report* shows a complex trough of low pressure over England and Wales with a shallow depression centred over the Cherbourg peninsula and a ridge extending over Ireland from the west.

him to place me at 2,000 feet altitude, to regain the N. $\frac{1}{2}$ W. current, and we then came in view of Crewkerne. I now kept at a low altitude until I reached Beaminster. Mr. Powell here observed that we were going at 30 miles an hour, and here we first heard the roar of the sea. The balloon suddenly rose to 4,000 feet. At this time I said to Mr. Powell, "Go down to within 100 feet of the earth and ascertain our exact position." We coasted along close to the ground until we reached Symondsbury. I here called to a man and asked him how far the distance was to Bridport, and he said about a mile. I asked Mr. Powell to prepare to "take in;" our pace now increasing to 35 miles an hour. To avoid the little village of Eype, Mr. Powell threw out some ballast. This took us to 1,500 feet elevation and we had still two miles to get in. I opened the valve and descended about 150 yards short of the cliff. The balloon on touching the ground dragged a few feet, and I rolled out of the car with the valve line in my hand. This caused the balloon to ascend about 8 feet, when Mr. Gardner dropped off, and unfortunately broke his leg. I found that the rope was being pulled through my hands, and I called to Mr. Powell, who was standing in the car, to come down the line. He took hold of the line, and in a few more seconds the line was torn through my hands. The balloon rose rapidly. Mr. Powell waved his hand to me, and I took his compass bearings, and found that he was going in a S. $\frac{1}{2}$ E. direction. Some men coming up, I placed Mr. Gardner in their charge and sent word to the Coastguard and Bridport Harbour-master to keep a good look out, and to go out with boats. I then proceeded to Bridport and telegraphed to the Commanding Officer, Royal Engineers, Weymouth, to have a steamer in readiness for me to go in search. I proceeded to Weymouth and found the S.S. "Commodore" with steam up. I here received a telegram from Bridport Harbour-master saying that a balloon had been seen to drop in the sea south of Bridport. I at once proceeded to sea, searched the alleged place of his descent, making due allowance for the wind and current. This proving unsuccessful, I crossed the Channel till we sighted the Casquets Light, and then returned in a N.W. direction, ultimately reaching Weymouth about 5h. a.m. on Sunday morning, and have organised further search. I am of opinion that what was seen to fall into the sea was not the balloon, but part of the gear, thrown out to lighten the balloon, as the balloon could not have fallen so close to the shore as to be visible at about 5h. p.m.

I have, &c.

(Signed) JAMES TEMPLER,

Captain 7th Batt. King's Royal Rifle Corps.

R. H. Scott, Esq., F.R.S.,
Secretary, Meteorological Office.

The full account referred to above gives various observations and instrumental readings as well as additional details of the final disaster. Mr Powell was an expert and fearless aeronaut and had made more than 20 ascents in 1881; it seems from Captain Templer's account that he could possibly have saved himself by jumping out of the car, which was no more than eight feet from the ground, but perhaps he hoped to be able to land in France and save the balloon as well.

This tragedy brought an effective end to the use of manned balloons for the experimental investigation of the upper air, and development work was concentrated on the making of self-recording instruments to be carried by unmanned balloons and kites.

(Source: Minutes of the Proceedings of the Meteorological Council; 1879, 1880, 1881.)

Reviews

The glaciation of the Ecuadorian Andes, by Stefan Hastenrath. 160 mm \times 230 mm, pp. xiv + 159, illus. A. A. Balkema, Rotterdam, Netherlands, 1981. Price Hfl 50.00, £10.00.

This attractive book describes the glacial history of the Ecuadorian Andes from the Late Pleistocene to the present, mainly concentrating on present conditions and changes documented in the past few centuries. It will serve as a valuable reference in its area because of its abundant maps, photographs and tabulations of historical sources (which will benefit multilingual readers most). The recent and continuing recession of the Ecuadorian glaciers is shown in the final chapter to be paralleled by recession in tropical glaciers elsewhere in tropical America, Africa and Papua New Guinea.

Although in Chapter 3 the author describes the atmospheric circulation and climate of northern South America, no attempt is made to relate recent glacial changes to any observed long-term meteorological fluctuations that may have taken place. Knowing the complexities of influences on glaciers, the

author instead wisely proposes an observation program of glacial heat and mass budget measurements; but at least a listing of available standard meteorological data would be useful for those who might try to relate glacial recession to regional changes of temperature, precipitation and insolation.

The book is a useful contribution to the documentation of world climate and related features: the publication of books of similar quality on other tropical mountain glaciations would be welcomed.

D. E. Parker

Earth's aura: a layman's guide to the atmosphere, by Louise B. Young. 127 mm × 194 mm, pp. xi + 320, illus. Penguin Books Ltd, Harmondsworth, Middlesex, 1980. Price £2.50 (paperback), £7.50 (hardback).

The sub-title of this book clearly explains its nature and purpose. It is on the whole a good piece of scientific journalism by an author who is scientifically qualified herself, with research experience at M.I.T., has planned and edited several books of readings for adult education in science, and has been careful to seek the help and advice of acknowledged experts.

Topics dealt with include man's exploration of the atmosphere; the formation of rain, snow and hail; the circulation of chemical elements and compounds; man-made pollution; atmospheric wind-systems; optical effects; cosmic rays; the atmospheres of other planets; and climatic change and variability.

The book has a wealth of interesting quotations from the writings of eminent scientists such as Pascal, Newton, Franklin and Glaisher, diarists and writers such as Evelyn and Dana, glider pilots, and travellers and explorers; these give a feeling of immediate appreciation of the phenomena described as well as a sense of historical development. (The relationship between Descartes, Pascal, Périer, and the proposal and execution of the famous experiment on the Puy-de-Dôme is, however, much more complicated and murky than one would imagine from Mrs Young's rather starry-eyed account. See Middleton's *History of the barometer*, 1964.)

The general attitude is perhaps a little too uncritical: 'Some meteorologists believe that the presence of this [meteor] dust in our atmosphere affects the earth's rainfall'; perhaps some do, but many more do not. The style occasionally boils over into journalese; for example, in speaking of 1976, 'widespread fires raged uncontrolled through forests in France and Britain'; the fires of 1976, though serious, would have been much worse had it not been for the efforts of the fire brigades who, in the circumstances, succeeded remarkably well. Even—or perhaps especially—in a book for laymen, to say merely that the distances of the planets from the sun 'are not to scale' when the relevant diagram (Fig. 10) shows Pluto nine times as far from the sun as Mercury instead of 100 times is unnecessarily misleading; a simple list with actual distances would have been better.

R. P. W. Lewis

Notes and News

New Naval Liaison Officer

We are pleased to welcome Commander David Philpott, R.N., to the Meteorological Office where he has recently taken over from Commander A. S. Watt as the Naval Liaison Officer. Previously Commander Philpott was Officer in Command of the Royal Navy's School of Meteorology and Oceanography. Unfortunately, he has not brought his escort with him to Bracknell. (See Plate IV.)

THE METEOROLOGICAL MAGAZINE

No. 1313

December 1981

Vol. 110

CONTENTS

	<i>Page</i>
High-vorticity regions in rotating thermally driven flows. R. Hide, F.R.S.	335
Meteosat water vapour imagery. J. R. Eyre	345
One hundred years ago: a ballooning tragedy. R. P. W. Lewis	352
Reviews	
The glaciation of the Ecuadorian Andes. Stefan Hastenrath. <i>D. E. Parker</i>	353
Earth's aura: a layman's guide to the atmosphere. Louise B. Young. <i>R. P. W. Lewis</i>	354
Notes and news	
New Naval Liaison Officer	354

NOTICES

It is requested that all books for review and communications for the Editor be addressed to the Director-General Meteorological Office, London Road, Bracknell, Berkshire RG12 2SZ and marked 'For Meteorological Magazine'.

The responsibility for facts and opinions expressed in the signed articles and letters published in this magazine rests with their respective authors.

Applications for postal subscriptions should be made to HMSO, PO Box 569, London SE1 9NH.

Complete volumes of 'Meteorological Magazine' beginning with Volume 54 are now available in microfilm form from University Microfilms International, 18 Bedford Row, London WC1R 4EJ, England.

Full-size reprints of out-of-print issues are obtainable from Johnson Reprint Co. Ltd, 24-28 Oval Road, London NW1 7DX, England.

Please write to Kraus Microfiche, Rte 100, Millwood, NY 10546, USA, for information concerning microfiche issues.

© Crown copyright 1981

Printed in England by Heffers Printers Ltd, Cambridge
and published by
HER MAJESTY'S STATIONERY OFFICE

£1.80 monthly

Annual subscription £23.80 including postage

Dd. 716670 K15 12/81

ISBN 0 11 726289 7
ISSN 0026-1149